Macromolecular Chemistry and Physics
www.mcp-journal.de

Selective Metal-Complexation on Polymeric Templates and Their Investigation via Isothermal Titration Calorimetry

*Thomas Bätz, Marcel Enke, Stefan Zechel, Martin D. Hager, and Ulrich S. Schubert**

Selective complexation of metal ions represents a powerful tool for the development of versatile supramolecular architectures. While research in the field of molecular devices and machinery is sophisticated, the selective formation of metal complexes is not prevalent in polymer chemistry. Thus, the implementation of orthogonal binding concepts into a polymeric matrix is presented. In this context, an end-functionalized poly(*N*-isopropylacrylamide) (PNIPAm) carrying zinc-porphyrin (ZnTPP) as well as a terpyridine (tpy) ligand side by side is utilized. With these binding sites, the polymer can simultaneously interact with a pyridine moiety via a ZnTPP interaction and a terpyridine unit by the formation of a bis-terpyridine complex. The complexation behavior of this polymer and different model compounds is intensively investigated by isothermal titration calorimetry. The obtained results indicate that the reported orthogonality of these two systems is successfully transferred into a functional polymeric architecture.

1. Introduction

The selective complexation behavior of metal ions has been of great interest for a long time. It is typically explored in nature, where living organisms can complex metal ions highly selectively.[1] Metal complexes are playing a key role in biological processes; however, metal ions can also be harmful to organisms in case of a too high concentration.[2] Thus, several approaches have been investigated in order to bind and remove metal ions from aqueous solutions,[3] also including ligand-containing polymers.[4,5] Beside the purification of water, selective complexation can be utilized for more advanced applications. The field of supramolecular self-assembly, based on coordination, has expanded rapidly in the last decades,[6,7] culminating in the development of molecular switches, devices, and machines.[8,9] Thus, special molecular geometries could be obtained, e.g., it was also possible to create dendrimers and metallocages.[10–12] The incorporation of orthogonal binding concepts can be a powerful tool in this context.[13] This approach can be based on either different[14] or even the same kind of supramolecular interaction.[15] Some of these approaches utilized the heteroleptic formation of complexes, thus, the binding of different ligands to one metal center. The most frequently used concepts are HETeroleptic *bis*-PHENanthroline (HETPHEN),[16] HETeroleptic Terpyridine And Phenanthroline (HETTAP)[17] and HETeroleptic PYridine and Phenanthroline (HETPYP),[18] which were developed over the years and can be widely applied for the selective combination of different counterparts. For the selective formation of complex supramolecular architectures, which are based on more than one concept, orthogonality between the concepts is the prerequisite. This orthogonality could already be shown in several studies.[19,20] In particular the pyridine to zinc(II)–porphyrin (ZnTPP) complexation was found to be very useful in this context.[21,22] The ZnTPP provides only one free axial binding site and multidentate ligands like terpyridine are not able to interact with ZnTPP due to steric constraints.

Even if terpyridine could theoretically coordinate the Zn(II) surrounded by porphyrin with one donor atom, this would lead to two uncoordinated donor sites, which is not compatible with the principle of maximum site occupancy.[22]

Nevertheless, these concepts are up to now exclusively utilized for the formation of supramolecular systems starting from small/low molar mass building blocks. The combination with polymers can enhance the field significantly resulting in new highly functional polymers. The combination of the selective binding sites with polymeric backbones can enable an additional way to tune the properties of such systems. In this context, the development of heterogeneous as well as homogeneous systems with desired solubility attributes is imaginable. In addition, the solubility of these systems can be switched easily, which was utilized for instance for polymer-assisted solution-phase synthesis.[23] Furthermore, the combination of selective complexation and macromolecules could also lead to potential new functional materials, such as self-healing or shape-memory polymers.[24]

T. Bätz, M. Enke, S. Zechel, M. D. Hager, U. S. Schubert
Laboratory of Organic and Macromolecular Chemistry (IOMC)
Friedrich Schiller University Jena
Humboldtstr. 10, Jena 07743, Germany
E-mail: ulrich.schubert@uni-jena.de
T. Bätz, M. Enke, S. Zechel, M. D. Hager, U. S. Schubert
Jena Center for Soft Matter (JCSM)
Friedrich Schiller University Jena
Philosophenweg 7, Jena 07743, Germany

The ORCID identification number(s) for the author(s) of this article can be found under https://doi.org/10.1002/macp.202100295

DOI: 10.1002/macp.202100295

Hence, in this study, the implementation of already published orthogonal binding concepts into a polymeric system was used to achieve a general proof of principle of selective complexation on polymeric templates. The complexation behavior of such multicomponent supramolecular systems has often been investigated by NMR spectroscopy.[25] In the case of polymeric templates, this method is less suitable due to the challenging interpretation of NMR spectra of polymeric systems.[26] In particular, when it comes to metallopolymers with paramagnetic ions the acquisition of conclusive NMR spectra is not possible anymore. As a consequence, the selective complexation was monitored by isothermal titration calorimetry (ITC) in our case. This technique represents a powerful tool for the investigation of the complexation behavior, since it provides information about precise stoichiometric ratios and thermodynamic values like binding affinities, also for macromolecular systems with various binding sites.[27]

2. Results and Discussion

2.1. Synthesis

In order to investigate the strategy of selective complexation in a polymeric structure, an end-functionalized polymer with two different ligand moieties has to be synthesized first. This polymer should act as a template for the complexation of unequal ligand counterparts. As complexation motifs, the pyridine → ZnTPP interaction as well as a simple bis-terpyridine complex formation with zinc(II) as central ion was chosen. This combination is well-established in the field of selective complexation and should be possible without any undesired cross-interactions due to the orthogonality between the N → ZnTPP concept and other complexes based on multidentate ligands.[28] PNIPAm was utilized as polymeric backbone, which is commercially available as monofunctional amine and, thus, can be functionalized with established amide coupling chemistry.

Two general principles are imaginable for the synthesis of the desired polymeric template. On the one hand, the step-by-step end functionalization of the polymer backbone is possible. The second pathway could be an end functionalization of the polymer with a presynthesized reagent bearing both ligand moieties. In this study, the second approach was chosen, which promises easier purification and analysis between the single synthetic steps. First, a suitable linker was required to covalently link the different building blocks. For this purpose, a commercially available glutamic acid derivate bearing a fluorenylmethoxycarbonyl (Fmoc) and a *tert*-butyloxycarbonyl (Boc) protecting group, Fmoc-Glu(OtBu)-OH, was chosen. This molecule carries three functional groups, which are partially protected and, thus, are orthogonally accessible for carbodiimide coupling reactions. The complete synthetic pathway is shown in **Scheme 1**. First, the porphyrin building block (4-(10,15,20-triphenylporphyrin-5-yl)aniline) was attached to the free carboxylic acid group of the glutamic acid linker. Therefore, a simple reaction setup using dicyclohexylcarbodiimide (DCC) as coupling reagent and CH_2Cl_2 as solvent was utilized. The reaction was carried out under inert conditions due to the strong tendency of carbodiimide compounds to decompose in the presence of water.

The usage of the glutamic acid as monohydrate can cause problems in this context. This was solved by the utilization of two equivalents of DCC for an in situ dehydration of the reagents. The arising by-product dicyclohexylurea (DCU) is insoluble in dichloromethane and could be filtered off after the reaction. Subsequently, the coupling product was deprotected using piperidine in dimethylformamide (DMF). The resulting substance (**2**) carried a free amino group utilized for the coupling reaction with a terpyridine containing carboxylic acid, which was previously synthesized according to a literature procedure.[29] For this coupling step, the previously used setup including only DCC was not applicable anymore. First attempts revealed low conversions and the dominant formation of side-products. A combination of diisopropylcarbodiimide (DIC) and OxymaPure revealed a significant higher yield.

The cleavage of the *tert*-butoxy protecting group of **3** was performed under acidic conditions with trifluoroacetic acid (TFA). Triethylsilane was utilized as a scavenger. In this synthesis, a color change from dark violet to green was observable, which was caused by a protonation of the porphyrin. To remove the excess of the acid and to deprotonate the porphyrin to its original state the solution was washed with saturated $NaHCO_3$. Another color change back to violet indicates the success of this procedure. The resulting product could not be characterized by NMR spectroscopy. Several approaches using different solvents and concentrations led to inconclusive spectra with very broad signals. This may be caused by the aggregation of the compound in the presence of a free carboxylic acid. Consequently, support for the successful conversion was obtained by HR ESI-TOF MS and the violet solid was utilized without further purification.

For the end-functionalization of $PNIPAm_{2000}$-NH_2 with compound **4**, an improved coupling approach using hydroxybenzotriazole (HOBt) as additional coupling agent was found to be effective. Compound **4** was utilized in slight excess to ensure a complete functionalization of the polymer. The surplus reagent and side products were easily removable by column chromatography utilizing neutral alumina as stationary phase. To prepare the Zn(II)-porphyrin moiety, **P1** was treated with $Zn(OAc)_2$ under heating to reflux. To achieve a quantitative metalation, the Zn(II)-salt was utilized in excess. Beside the metalation, this excess is leading to complexation of Zn(II) ions to the terpyridine unit.

Therefore, the crude product was washed with a disodium ethylenediamine tetraacetic acid (Na_2EDTA) solution leading to the polymeric template **P2**. The comparison of specific regions of the ^1H NMR spectra of **P1** and **P2** (**Figure 1**b) indicates the success of this procedure. The terpyridine signals (red) remained unshifted, which indicates no metal complexation, while the NH-signal of the porphyrin core (blue) at negative ppm values disappeared completely.

The SEC traces of the polymers (Figure 1a) verify a functionalization of PNIPAm. **P1** as well as **P2** feature significant shifts towards higher molar masses and no shoulder was observed indicating the absence of unfunctionalized polymer. Nevertheless, a slight difference between the SEC-traces of **P1** and **P2** can be observed even if the molar mass change during the metalation is very small. Both functionalized polymers also feature a signal using the diode array detector (DAD), while the PNIPAm-NH_2 is not detectable (Figure S9, Supporting Information). Thus, the SEC measurements are indicating a successful functionalization. The SEC evaluation revealed a molar mass for **P2** of

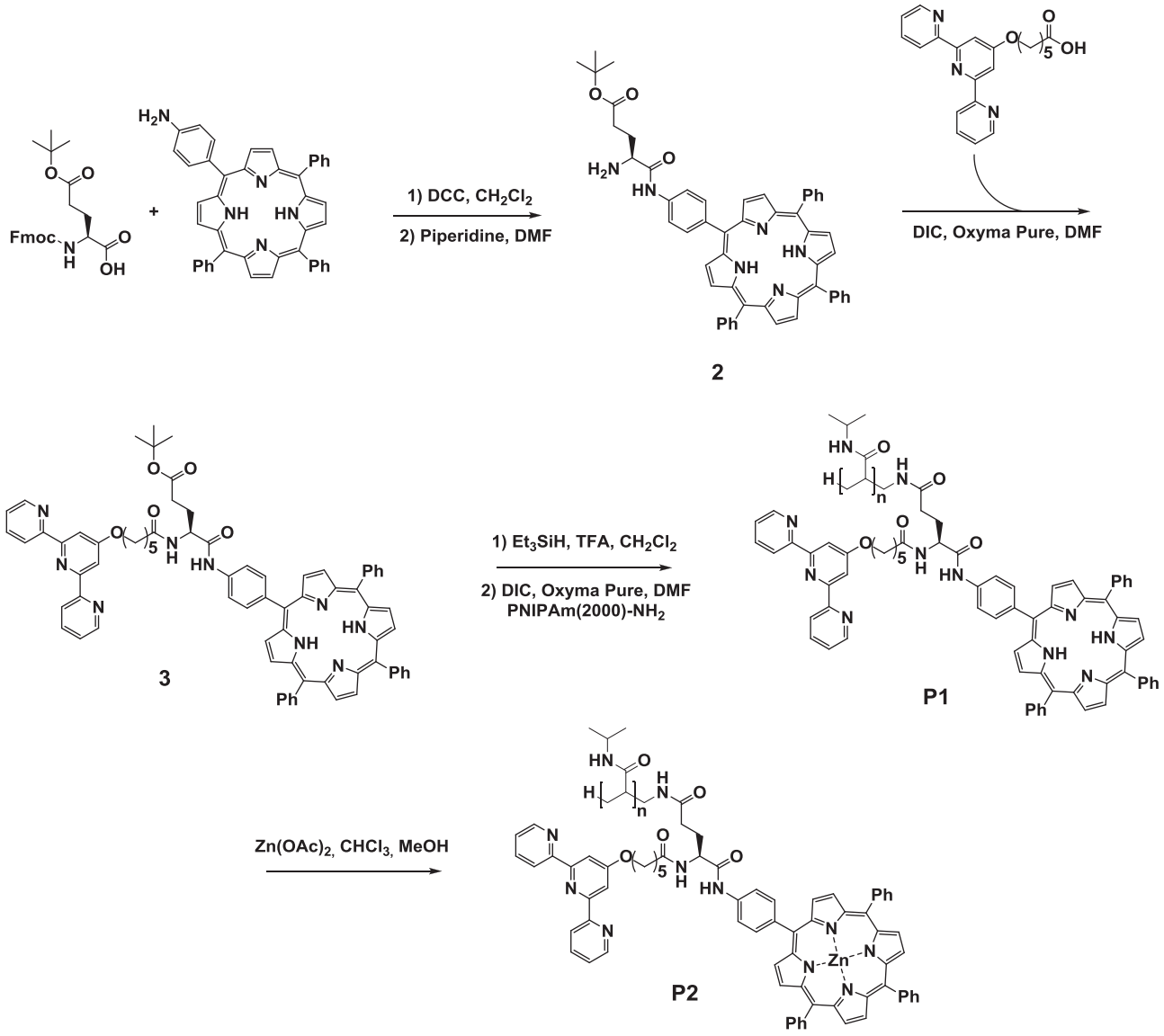

Scheme 1. Schematic representation of the synthesis of the polymeric template **P2**.

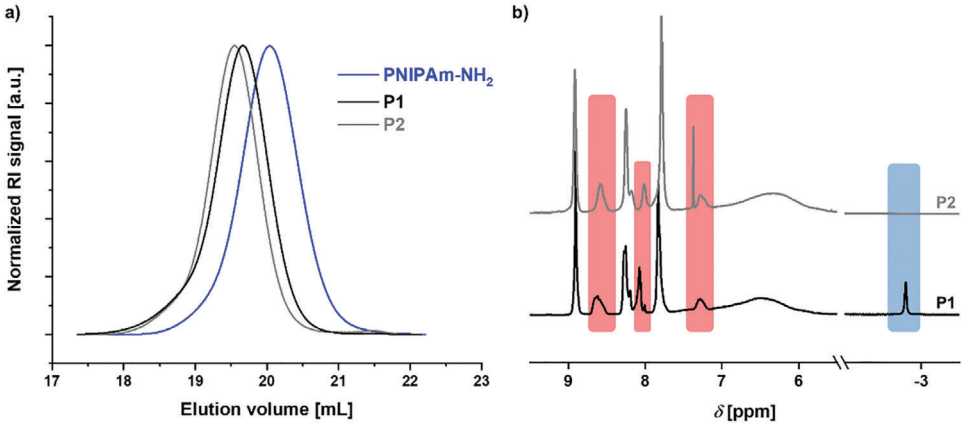

Figure 1. a) SEC-traces of PNIPAM-NH_2 (blue), **P1** (black) and **P2** (gray) (DMAc + 0.21% LiCl, RI detector, PMMA standard). b) Zoom of the ^{1}H NMR spectra of **P1** (black) and **P2** (gray) (250 MHz, CD_2Cl_2).

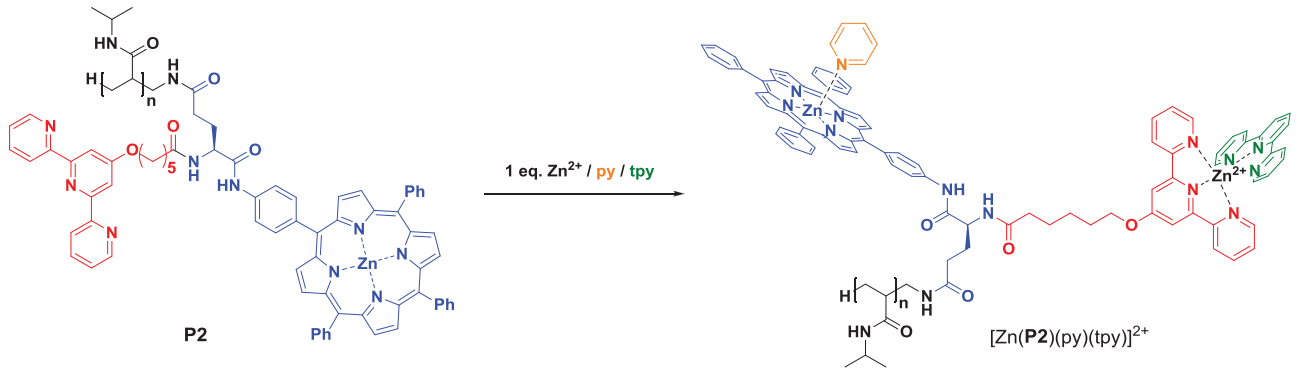

Scheme 2. Schematic representation of the selective complexation of the ligands py and tpy at the polymeric template **P2**.

$M_n = 7600$ g mol^{-1}, which is higher than the expected theoretical value of 3104 g mol^{-1} (calculated for 17 repeating units PNIPAm) based on the starting materials.

This finding can presumably be explained by the polarity difference between PNIPAm and the PMMA standard, in particular after the introduction of polar end groups, which can change the behavior of the polymer in solution significantly. Nevertheless, to enable precise ITC investigations, accurate values for M_n of **P2** are required. For this purpose, the template was characterized by MALDI-TOF MS (Figure S8, Supporting Information). The maximum of the [**P2**+Na]$^+$ distribution turned out to be equal to the theoretical value, calculated for 17 repeating units. Hence, the molar mass M_n = 3104 g mol^{-1} was utilized for the polymeric template for the following investigations.

2.2. Investigation of Selective Complexation

Due to the orthogonality between the N → ZnTPP interaction and concepts based on multidentate ligands, the addition of an equimolar mixture of a Zn^{2+}-salt, pyridine (py) and terpyridine (tpy) to the polymer **P2** should lead to a selective formation of a py → ZnTPP moiety beside a *bis*-tpy zinc complex (**Scheme 2**).[30]

To investigate this behavior in more detail and to verify the previous assumption, several ITC measurements were performed. These measurements include fundamental titrations with the metal salt ($ZnOTf_2$), unfunctionalized model compounds and titrations of the template. The obtained results are summarized in **Table 1**. Due to the potential of PNIPAm to interact with metal centers,[31] a test-titration with the unfunctionalized polymer was also performed (ITC-1). This experiment resulted in an endothermic complexation of Zn^{2+} by PNIPAm with a K_α (10^4) two orders of magnitude smaller compared to the ones for a tpy → Zn^{2+} complexation (10^6). Thus, the polymer backbone should not interfere with the tpy binding motif.

To demonstrate the formation of the desired motif in solution, $ZnOTf_2$ was titrated with tpy (ITC-2). The titration revealed one transition at a molar ratio of 2:1, which represents the expected formation of a homoleptic octahedral *bis*-tpy complex $[Zn(tpy)_2]^{2+}$. The inverse experiment (ITC-3) resulted in an exothermic transition at a molar ratio of 0.5:1 with an association constant (K_α) comparable to the one observed in ITC-2, which shows the formation of the same species as in ITC-2. Additionally, this is directly followed by an endothermic process representing the decomposition of the stable *bis*-tpy complexes. Since this process could be found at a molar ratio of 0.6:1 instead of 1:1, a decomposition to *mono*-tpy species $[Zn(tpy)]^{2+}$ can be excluded. Instead, the formation of higher supramolecular structures including multiple metal centers featuring bridging tpy ligands seems to a potential explanation. Additionally, the Zn porphyrin moiety (**M2**) was titrated with py (ITC-4). In first attempts, no complexation reaction could be observed using the commonly used solvent mixture of MeOH:$CHCl_3$ 2:1.[32] This result is maybe attributed with the low solubility of **M2** in MeOH, which only enables measurements with low concentrations. Furthermore, MeOH can potentially coordinate the Zn(II) in **M2**, which would hinder a complexation by py. Performing the titration in pure $CHCl_3$ seemed to be a suitable method and a weak interaction at a molar ratio of 1:1 could be observed. This finding indicates the formation of the N → Zn porphyrin binding.

Table 1. Results of ITC measurements for **P2**.

Entry	Cell	Syringe	Solvent	n (s/c)[a]	K_α
ITC-1	PNIPAm-NH_2	$ZnOTf_2$	$CHCl_3$/MeOH 1/2	0.43	7.62×10^4[c]
ITC-2	$ZnOTf_2$	Tpy	$CHCl_3$/MeOH 1/2	1.90	3.24×10^6
ITC-3	Tpy	$ZnOTf_2$	$CHCl_3$/MeOH 1/2	0.51 0.58	6.52×10^6 1.35×10^7[c]
ITC-4	**M2**	Py	$CHCl_3$	1.14	9.07×10^2
ITC-5	**M1**	Py	$CHCl_3$/MeOH 1/2	–[b]	–
ITC-6	**M2**	Tpy	$CHCl_3$	–[b]	–
ITC-7	**P2**	$ZnOTf_2$	$CHCl_3$/MeOH 1/2	0.29 0.41	3.62×10^7 1.63×10^6[c]
ITC-8	$ZnOTf_2$/ **P2** 1/1	tpy	$CHCl_3$/MeOH 1/2	1.00 1.11	5.46×10^5[c] 1.88×10^6
ITC-9	$ZnOTf_2$ / tpy 1 / 1	tpy	$CHCl_3$/MeOH 1/2	0.78 0.87	4.28×10^5[c] 8.92×10^5
ITC-10	**P2**	py	$CHCl_3$	0.77	2.93×10^3
ITC-11	$ZnOTf_2$ / **P2** / py 1 / 1 / 1	tpy	$CHCl_3$/MeOH 1/2	0.99 1.19	5.18×10^5[c] 8.31×10^5
ITC-12	ZnOTf2 / **P2** / tpy 1 / 1 / 1	py	$CHCl_3$	0.96	1.10×10^3

[a] Molar ratio (syringe/cell); [b] no complexation observed; [c] endothermic process.

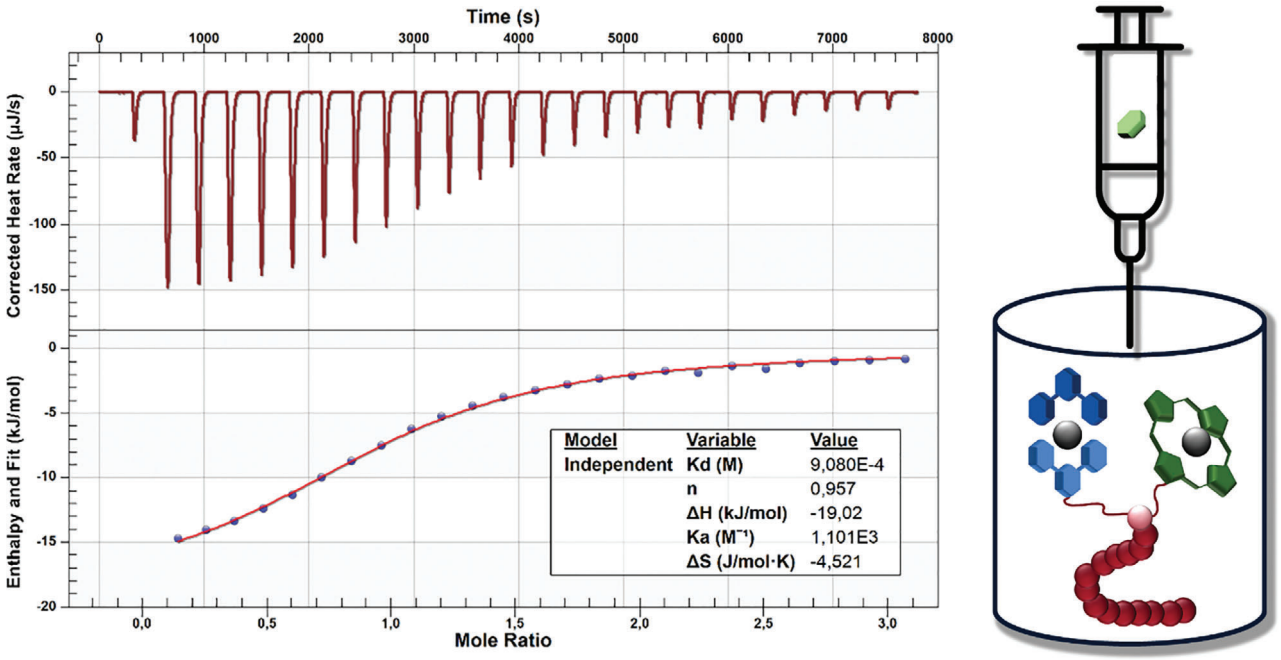

Figure 2. ITC titration data of **P2** / $Zn(OTf)_2$ / tpy (in cell) with py (in syringe) (**ITC-12**) and schematic representation of the experimental setup.

To prove the orthogonality between the two complex motifs, the model compounds $[Zn(tpy)_2]OTf_2$ (**M1**) and ZnTPP (**M2**) were titrated with the competing counterpart, py or tpy, respectively. Both experiments (ITC-5 and 6) indicated no complexation or interaction, which proves the orthogonal binding concept.

The titration of **P2** with $ZnOTf_2$ (ITC-7) should only address the tpy ligand of the template and, thus, a similar result as for ITC-2 was expected, which could be found (Figure S18, Supporting Information). The first exothermic complexation (formation of $[Zn(tpy)_2]^{2+}$ between two template molecules) appears at a molar ratio of approximately 0.3:1, which is lower than the expected 0.5:1. This finding is presumably associated by a steric hindrance of the bulky functionalization of the tpy moieties and shielding effects of the polymer backbone. The following endothermic process appears slightly retarded compared to the model complexes. This indicates that the debonding of tpy dimers is overlapped by the simultaneous complexation of Zn-ions by the PNIPAm backbone (ITC-1). Thus, the transition at a molar ratio of approximately 0.4:1 seems to be an overlap of both processes. Furthermore, the template **P2** was mixed with $ZnOTf_2$ in a ratio of 1:1 and titrated with tpy (ITC-8). The titration curve can be viewed as an inverse representation of ITC-3 for the polymer. First of all, an endothermic process can be observed indicating the deformation of previously formed supramolecular structures. Directly after this signal, an exothermic transition at a molar ratio of approximately 1:1 could be revealed representing the formation of the $[Zn(\mathbf{P2})(tpy)]^{2+}$ *bis*-tpy complex. The same titration curve could be observed for the nonpolymeric model system (ITC-9; titration of tpy:Zn 1:1 with tpy) showing that the polymer does not influence the complexation of the ligands. Furthermore, the obtained binding strengths are comparable for the polymer and the nonpolymeric model system.

Nevertheless, these findings do not finally exclude the formation of undesired combinations like $([Zn(tpy)_2]^{2+}$ and $[Zn(\mathbf{P2})_2]^{2+})$. Consequently, DOSY-NMR experiments were performed to examine the presence of different species in the solution. The DOSY-NMR spectrum of $[Zn(\mathbf{P2})(tpy)]^{2+}$ (Figure S24a, Supporting Information) indicates the presence of only one polymeric species ($D \approx 1.65 \times 10^{-6}$) as well as a second species bearing only tpy-signals ($D \approx 3.40 \times 10^{-6}$). The diffusion coefficient of the polymer dimer $[Zn(\mathbf{P2})_2]^{2+}$ was determined ($D \approx 1.40 \times 10^{-6}$ (Figure S24b, Supporting Information).

Thus, this species is not visible in the DOSY-spectrum of $[Zn(\mathbf{P2})(tpy)]^{2+}$ (Figure S24a, Supporting Information) indicating the absence of $[Zn(\mathbf{P2})_2]^{2+}$ and, consequently, proving the selective formation of the desired $[Zn(\mathbf{P2})(tpy)]^{2+}$. The surplus tpy-species may be induced by a slight excess of tpy ligands traced back to weighing errors in the preparation of the equimolar mixture. The N → ZnTPP binding motif could also be generated at the template. For this purpose, **P2** was titrated with py (ITC-10). The evaluation revealed a weak interaction comparable to the results of the model titration (ITC-4). To finally combine the two binding motifs and prove the formation of the desired supramolecular structure (Scheme 2) each titration to address a template binding site had to be repeated in the presence of the competing counterparts. The complexation of a tpy ligand at the tpy binding site of **P2** using a zinc(II) metal center was monitored in the presence of an additional py ligand (ITC-11). The titration curve appears almost identical to ITC-9 with similar binding constants indicating that the py counterpart does not interfere into the formation of a $[Zn(tpy)_2]^{2+}$ complex at **P2**. Nevertheless, it does not ensure that the py → ZnTPP interaction is not influenced under these conditions. To investigate this, a preformed template species $[Zn(\mathbf{P2})(tpy)]^{2+}$ was titrated with py (ITC-12).

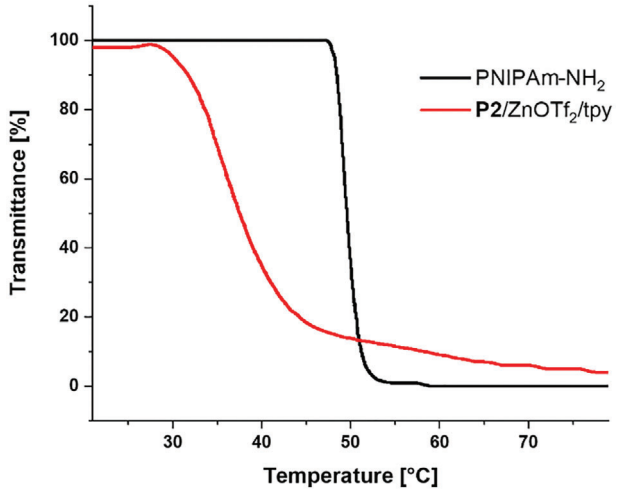

Figure 3. First heating run of turbidimetric characterization of PNIPAm-NH_2 (black, 2.57×10^{-3} M) and **P2**/ $Zn(OTf)_2$ / tpy (red, 1.40×10^{-3} M) in water.

The evaluation revealed a single complexation at a molar ratio of approximately 1:1 with a K_α similar to ITC-4 and ITC-10. Consequently, the py → ZnTPP complexation at **P2** is not affected by the presence of a *bis*-tpy complex.

Consequently, the ITC investigations revealed that the chosen binding motifs, a $[Zn(tpy)_2]^{2+}$ complex as well as the interaction between a py ligand and a metalated porphyrin, can be generated at the synthesized polymer template **P2** (ITC-9 and 10). Furthermore, the orthogonality between the two supramolecular interactions is shown through the titration of model compounds (ITC-5 and 6) as well as at the polymer itself (ITC-11 and 12; see **Figure 2**). The desired supramolecular structure combining both concepts (Scheme 2) could be generated by a stepwise formation of both motifs. According to the obtained results, the order of these steps does not have any influence on the success of the approach.

2.3. Investigation of the LCST Behavior

The utilization of the thermoresponsive PNIPAm as polymeric backbone introduces an additional feature to the template system. PNIPAm is well-known for its LCST behavior under moderate conditions in water.[33] Due to this property, it is of great interest in the fields of drug delivery as well as tissue engineering.[34]

In our case, this LCST behavior provides the potential to thermally switch between solution- or solid-phase-based template systems. The most established method to investigate the LCST behavior is turbidimetry, which directly provides the cloud point temperature (T_{cp}) under certain conditions.[35] Thus, we utilized this method to investigate the starting polymer (PNIPAm-NH_2) as well as the final template system. The results are displayed in **Figure 3** and Figure S25 (Supporting Information).

For the unfunctionalized polymer PNIPAm-NH_2 a T_{cp} of 49.6 °C could be determined. This value highly exceeds 32 °C, which is typically reported for PNIPAm.[36] This finding is based on the low molar mass of the polymer (2000 g mol^{-1}) as well as the amino end group inducing a solubilizing effect in water. Both characteristics increase the T_{cp}.[37] The functionalization of this polymer with a large hydrophobic group drastically decreases the T_{cp} even though a tpy-Zn complex is formed at the template **P2**. A T_{cp} of 37.4 °C was determined in this case. The precipitation of this sample is irreversible under the applied measurement conditions. Subsequent cooling to 20 °C does not dissolve the sample again (Figure S25, Supporting Information). This finding further demonstrates the hydrophobic influence of the end group.

3. Conclusion

In this study, a general first proof of principle of selective complexation in polymeric materials was achieved. For this purpose, a polymeric template based on a PNIPAm backbone was synthesized containing two different ligand moieties as one end-group. This included a multi-step synthesis of a functionalization reagent.

The template bearing two different building blocks for different complex motifs (tpy and ZnTPP) was intensively investigated via ITC measurements. The two binding motifs as well as their combination were also studied by this method using low molar mass model systems. It turned out that both concepts can be validated by ITC titration. Furthermore, the already reported orthogonality between the N → ZnTPP interaction and a *bis*-tpy complex could be confirmed. When it came to the investigation of the desired binding motifs using the polymeric template **P2** the titration curves appeared equal to the corresponding model titrations. These findings indicate the formation of the py → ZnTPP as well as the $[Zn(tpy)_2]^{2+}$ complex at the polymeric template. This behavior was not influenced by the presence of the competing binding motif, which finally proved that the orthogonality remains even in a polymeric material.

In this context, a first general validation of the working principle of selective complexation using polymers could be achieved. This study demonstrates the feasibility of introducing selective binding concepts into functional polymers. The selective formation of several complexes at the same polymeric backbone can be the basis for numerous advanced applications. Thus, functional metallopolymers can be fine-tuned to certain properties. One potential application could be the generation of shape-memory metallopolymers using orthogonal supramolecular interactions.[38]

4. Experimental Section

5,10,15,20-tetraphenylporphyrin,[39] 4-(10,15,20-triphenylporphyrin-5-yl)aniline,[40] and 6-([2,2“:6”,2“”-terpyridin]-4’-yloxy)hexanoic acid[29] were synthesized according to already published procedures. A detailed list of the used materials and instrumentation can be viewed in the Supporting Information.

Synthesis of the Polymeric Template: *Tert-butyl (S)-4-((((9H-fluoren-9-yl)methoxy)carbonyl)amino)-5-oxo-5-((4-(10,15,20-tri–phenylporphyrin-5-yl)phenyl)amino)pentanoate* (***1***):

4-(10,15,20-Triphenylporphyrin-5-yl)aniline (0.50 g, 0.79 mmol) and (*S*)-2-((((9*H*-fluoren-9 yl)methoxy)-carbonyl)amino)-5-(*tert*-butoxy)-5-oxopentanoic acid monohydrate (0.33 g, 0.75 mmol) were dissolved under nitrogen in 40 mL dry dichloromethane. Afterwards, DCC (0.31 g, 1.50 mmol), dissolved in 10 mL dry dichloromethane, was added and the mixture was stirred 23.5 h at RT. Subsequently, the reaction mixture was filtered, and the solvent was evaporated under reduced pressure.

The crude product was purified by column chromatography (silica gel/ CH_2Cl_2 → CH_2Cl_2:MeOH, 9:1).

Yield: 0.75 g (0.72 mmol) as violet crystals, 96%

Melting point: 190 °C

^{1}H NMR (300 MHz, $CDCl_3$): δ = −2.75 (s, 2H, NH_{por}), 1.48 (s, 9 H, CH_3), 2.10–2.25 (m, 1 H, CH_2), 2.30–2.45 (m, 1 H, CH_2), 2.50–2.65 (m, 1 H, CH_2), 2.65–2.80 (m, 1 H, CH_2), 4.31 (m, 1 H, C*H*), 4.45–4.65 (m, 3 H, CH_2, C*H*), 6.09 (d, 1 H, *J* = 6 Hz, N*H*), 7.30–7.48 (m, 4 H, *H*-aromatic), 7.65–7.72 (m, 2 H, *H*-aromatic), 7.73–7.85 (m, 11 H, *H*-aromatic), 7.95–8.05 (m, 2 H, *H*-aromatic), 8.15–8.30 (m, 8 H, *H*-aromatic), 8.80–8.95 (m, 8 H, *H*-aromatic), 9.12 (s, 1 H, N*H*) ppm.

^{13}C NMR (100 MHz, $CDCl_3$): δ = 25.6 (*C*H_2), 28.2 (*C*H_3), 34.0 (*C*H_2), 47.2 (*C*H), 67.4 (*C*H), 77.3 (*C*H_2), 81.7 (*C*$_q$), 118.2 (*C*-aromatic), 119.5 (*C*-aromatic), 120.0 (*C*-aromatic), 120.1 (*C*-aromatic), 120.2 (*C*-aromatic), 125.1 (*C*-aromatic), 126.7 (*C*-aromatic), 127.2 (*C*-aromatic), 127.7 (*C*-aromatic), 127.8 (*C*-aromatic), 134.6 (*C*-aromatic), 135.1 (*C*-aromatic), 137.4 (*C*-aromatic), 138.3 (*C*-aromatic), 141.4 (*C*-aromatic), 142.2 (*C*-aromatic), 143.7 (*C*-aromatic), 143.8 (*C*-aromatic), 156.8 (C═O), 170.0 (C═O), 173.6 (C═O) ppm.

ESI-TOF MS (HR MS): calc.: m/z = 1037.4385 $[M+H]^+$; found: m/z = 1037.4337 $[M+H]^+$; error: 4.6 ppm.

*Tert-butyl (S)-4-amino-5-oxo-5-((4-(10,15,20-triphenylporphyrin-5-yl)phenyl)amino)pentanoate (**2**)*:

Compound **1** (6.60 g, 6.36 mmol) was dissolved in 200 mL DMF. Afterward, 40 mL piperidine was added and the mixture was stirred 1 h at RT. Subsequently, the solvent was evaporated under reduced pressure. The crude product was purified by column chromatography (silica gel/ starting with CH_2Cl_2 changed to CH_2Cl_2:MeOH, 24:1). After solvent evaporation, the isolated fraction was dissolved in 150 mL toluene. The solution was filtered and evaporated under reduced pressure.

Yield: 3.83 g (4.70 mmol) as violet solid, 74%

Melting point: 218 °C

^{1}H NMR (400 MHz, $CDCl_3$): δ = −2.75 (s, 2H, NH_{por}), 1.48 (s, 9 H, CH_3), 2.30–2.50 (m, 2 H, CH_2), 2.65–2.80 (m, 4 H, CH_2, NH_2), 3.71 (m, 1 H, C*H*), 7.73–7.85 (m, 9 H, *H*-aromatic), 8.00–8.09 (m, 2 H, *H*-aromatic), 8.20–8.30 (m, 8 H, *H*-aromatic), 8.85–8.95 (m, 8 H, *H*-aromatic), 9.87 (s, 1 H, N*H*) ppm.

^{13}C NMR (100 MHz, $CDCl_3$): δ = 26.3 (*C*H_2), 28.2 (*C*H_3), 30.3 (*C*H_2), 55.4 (*C*H), 80.9 (*C*$_q$), 117.7 (*C*-aromatic), 119.6 (*C*-aromatic), 119.7 (*C*-aromatic), 120.1 (*C*-aromatic), 120.2 (*C*-aromatic), 125.5 (*C*-aromatic), 126.7 (*C*-aromatic), 127.0 (*C*-aromatic), 127.7 (*C*-aromatic), 134.6 (*C*-aromatic), 135.2 (*C*-aromatic), 137.5 (*C*-aromatic), 138.0 (*C*-aromatic), 141.0 (*C*-aromatic), 142.2 (*C*-aromatic), 146.7 (*C*-aromatic), 172.9 (C═O), 173.0 (C═O) ppm.

ESI-TOF MS (HR MS): found: m/z = 815.41 $[M+H]^+$.

*Tert-butyl (S)-4-(6-([2,2":6",2""-terpyridin]-4'-yloxy)hexanamido)-5-oxo-5-((4-(10,15,20-triphenylporphyrin-5-yl)phenyl)amino)pentanoate (**3**)*:

Compound **2** (0.22 g, 0.61 mmol) and 6-([2,2':6',2"-terpyridin]-4'-yloxy)hexanoic acid (0.50 g, 0.61 mmol) were dissolved under nitrogen in 20 mL dry DMF. The solution was cooled to 0 °C. Afterward, OxymaPure (0.09 g, 0.61 mmol), dissolved in 3 mL dry DMF, was added and the mixture was stirred 15 min at 0 °C. Subsequently, DIC (0.1 mL, 0.61 mmol) was added and the reaction mixture was stirred 2 h at 0 °C. The solution was allowed to warm up to RT and was stirred overnight (22 h). On the next day, the solvent was evaporated under reduced pressure. The residue was dissolved in chloroform, washed three times with 50 mL of deionized water and dried over Na_2SO_4. Subsequently, the solvent was evaporated under reduced pressure. The crude product was purified by flash column chromatography (neutral alumina/ starting with CH_2Cl_2:EtOAc, 7:3 changed to EtOAc).

Yield: 0.41 g (0.35 mmol) as violet solid, 58%

Melting point: 176 °C

^{1}H NMR (250 MHz, $CDCl_3$): δ = −2.76 (s, 2H, NH_{por}), 1.49 (s, 9 H, CH_3), 1.62–1.76 (m, 2 H, CH_2), 1.85–2.05 (m, 4 H, CH_2), 2.12–2.65 (m, 6 H, CH_2), 4.30 (t, 2H, *J* = 7.5 Hz, CH_2), 4.84 (m, 1H, C*H*), 7.02 (d, 1H, *J* = 7.5 Hz, N*H*), 7.15–7.25 (m, 2 H, *H*-aromatic), 7.65–7.85 (m, 11 H, *H*-aromatic), 7.95–8.07 (m, 4 H, *H*-aromatic), 8.15–8.35 (m, 8 H, *H*-aromatic), 8.41 (d, 2H, *J* = 10 Hz, *H*-aromatic), 8.61 (d, 2 H, *J* = 5 Hz, *H*-aromatic), 8.80–8.95 (m, 8 H, *H*-aromatic), 9.55 (s, 1 H, N*H*) ppm.

^{13}C NMR (75 MHz, $CDCl_3$): δ = 23.5 (*C*H_3), 25.3 (*C*H_2), 25.8 (*C*H_2), 28.1 (*C*H_2), 28.2 (*C*H_2), 28.8 (*C*H_2), 36.5 (*C*H_2), 42.2 (*C*H_2), 67.9 (*C*H), 81.5 (*C*$_q$), 107.4 (*C*-aromatic), 118.1 (*C*-aromatic), 119.6 (*C*-aromatic), 120.1 (*C*-aromatic), 121.2 (*C*-aromatic), 123.7 (*C*-aromatic), 126.7 (*C*-aromatic), 127.7 (*C*-aromatic), 134.5 (*C*-aromatic), 135.1 (*C*-aromatic), 136.7 (*C*-aromatic), 137.7 (*C*-aromatic), 138.1 (*C*-aromatic), 142.2 (*C*-aromatic), 148.9 (*C*-aromatic), 156.0 (*C*-aromatic), 157.0 (*C*-aromatic), 167.2 (*C*-aromatic), 170.0 (*C*-aromatic), 173.7 (*C*═O), 173.8 (*C*═O), 173.9 (*C*═O) ppm.

ESI-TOF MS (HR MS): calc.: m/z = 1160.4943 $[M]^+$; found: m/z = 1160.4960 $[M]^+$; error: −1.7 ppm.

*(S)-4-(6-([2,2":6",2""-Terpyridin]-4'-yloxy)hexanamido)-5-oxo-5-((4-(10,15,20-triphenylporphyrin-5-yl)phenyl)amino)pentanoic acid (**4**)*:

Compound **3** (2.05 g, 1.77 mmol) was dissolved in 200 mL dichloromethane. Afterwards, 50 mL TFA and triethylsilane (0.28 mL, 1.77 mmol) were added. The green solution was stirred overnight (20 h) at RT. Subsequently, the reaction mixture was concentrated under reduced pressure, diluted with chloroform and washed once with saturated aqueous $NaHCO_3$-solution and once with brine. The organic phase was dried over Na_2SO_4. The solvent was removed under reduced pressure. The product was used without further purification.

Yield: 1.95 g (1.77 mmol) as violet solid, 100%

ESI-TOF MS (HR MS): calc.: m/z = 1104.4317 $[M]^+$; found: m/z = 1104.4305 $[M]^+$; error: 1.2 ppm.

*Functionalization of PNIPAm$_{2000}$-NH$_2$ (**P1**)*:

Compound **4** (0.73 g, 0.66 mmol) and PNIPAm$_{2000}$-NH_2 (1.00 g, 0.50 mmol) were dissolved under nitrogen in 40 mL dry DMF. The solution was cooled to 0 °C. Subsequently, wetted hydroxybenzotriazole (0.15 g, 1.11 mmol), dissolved in 20 mL dry DMF, was added and the mixture was stirred 15 min at 0 °C. Afterward, DIC (0.45 mL, 2.91 mmol) was added and the reaction mixture was stirred 2 h at 0 °C. The solution was allowed to warm up to RT and was further stirred for 42 h. The solvent was evaporated under reduced pressure. The crude product was purified by flash column chromatography (neutral alumina/ starting with EtOAc changed to EtOAc:MeOH, 9:1).

Yield: 1.14 g (0.38 mmol) as purple solid, 75%

^{1}H NMR (250 MHz, CD_2Cl_2): δ = −2.84 (s, 2 H, NH_{por}), 0.70–2.60 (m, 166 H, *H*-backbone, CH_2), 3.60 (m, 2 H, N–CH_2) 3.80–4.15 (m, 17 H, N–C*H*), 4.20–4.35 (m, 3 H, C*H*, CH_2,), 5.60–7.10 (m, 17 H, N*H*), 7.15–7.30 (m, 2 H, *H*-aromatic), 7.65–7.85 (m, 13 H, *H*-aromatic), 7.90–8.00 (m, 5 H, *H*-aromatic, N*H*), 7.95–8.1 (m, 6 H, *H*-aromatic), 8.45–8.65 (m, 4 H, *H*-aromatic), 8.80–8.95 (m, 8 H, *H*-aromatic) ppm.

MALDI-TOF MS: M_n = 3360 g mol^{-1}, M_w = 3430 g mol^{-1}, $Đ$ = 1.02.

SEC (DMAc + 0.21% LiCl, RI detector, PMMA standard): M_n = 6500 g mol^{-1}, M_w = 7100 g mol^{-1}, $Đ$ = 1.10.

*Metalation of the Porphyrin Moiety (**P2**)*:

P1 (1.10 g, 0.36 mmol) and $Zn(OAc)_2 \times 2H_2O$ (0.27 g, 1.24 mmol) were dissolved in 60 mL $CHCl_3$:MeOH 2:1. The solution was heated to reflux for 3.5 h. Afterward, the solvent was evaporated under reduced pressure. The residue was dissolved in $CHCl_3$, washed once with saturated aqueous $NaHCO_3$ solution, three times with an aqueous Na_2EDTA solution (0.05 M) and twice with brine. The organic phase was dried over Na_2SO_4 and evaporated under reduced pressure. The crude product was purified by preparative size exclusion chromatography (BioBeads SX-1/ swollen in $CHCl_3$).

Yield: 1.07 g (0.35 mmol) as purple solid, 95%

^{1}H NMR (400 MHz, CD_2Cl_2): δ = 0.70–2.40 (m, 166 H, *H*-backbone, CH_2), 3.40 (m, 2 H, N–CH_2) 3.60–4.00 (m, 17 H, N–C*H*), 4.05–4.20 (m, 3 H, C*H*, CH_2,), 5.50–7.00 (m, 17 H, N*H*), 7.05–7.25 (m, 2 H, *H*-aromatic), 7.55–7.80 (m, 13 H, *H*-aromatic), 7.80–7.95 (m, 3 H, *H*-aromatic, N*H*), 7.95–8.25 (m, 8 H, *H*-aromatic), 8.35–8.60 (m, 4 H, *H*-aromatic), 8.70–8.95 (m, 8 H, *H*-aromatic) ppm.

MALDI-TOF MS: M_n = 3190 g mol^{-1}, M_w = 3250 g mol^{-1}, $Đ$ = 1.02.

SEC (DMAc + 0.21% LiCl, RI detector, PMMA standard): M_n = 7600 g mol^{-1}, M_w = 8200 g mol^{-1}, $Đ$ = 1.08.

Synthesis of Model Compounds: *[Zn(tpy)$_2$]OTf$_2$ (**M1**)*:

$ZnOTf_2$ (0.39 g, 1.07 mmol) and terpyridine (0.50 g, 2.14 mmol) were dissolved in 30 mL $CHCl_3$:MeOH 2:1 and stirred for 30 min at room temperature. Afterward, the solvent was evaporated under reduced pressure. The residual solid was dried *in vacuo* and characterized by ESI-MS and ^{1}H NMR spectroscopy.

Yield: 0.89 g (1.07 mmol) as yellow solid, 100%

^{1}H NMR (300 MHz, DMSO-d_6): δ = 7.40– 7.55 (m, 2 H, *H*-aromatic), 7.85 (d, 2H, *J* = 6 Hz, *H*-aromatic), 8.25 (t, 2 H, *J* = 6 Hz, *H*-aromatic), 8.75– 8.95 (m, 3 H, *H*-aromatic), 9.08 (d, 2H, J = 6 Hz, *H*-aromatic) ppm.

ESI-TOF MS: found: m/z = 265.06 $[M\text{-}2OTf]^{2+}$

5,10,15,20-Tetraphenylporphyrin[Zn] (ZnTPP) (M2):

5,10,15,20-Tetraphenylporphyrin (1.00 g, 1.59 mmol) and $Zn(OAc)_2 \times 2H_2O$ (1.22 g, 5.56 mmol) were dissolved in 250 mL $CHCl_3$:MeOH 2:1. The solution was refluxed for 3.5 h. Afterwards, the solvent was evaporated under reduced pressure. The crude product was purified by gel filtration (silica gel/ $CHCl_3$).

Yield: 1.02 g (1.50 mmol) as yellow solid, 94%

^{1}H NMR (300 MHz, CD_2Cl_2): δ = 7.75– 7.85 (m, 12 H, *H*-aromatic), 8.20– 8.30 (m, 8 H, *H*-aromatic), 8.98 (s, 8 H, *H*-aromatic) ppm.

^{13}C NMR (75 MHz, $CDCl_3$): δ = 121.1 (*C*-aromatic), 126.6 (*C*-aromatic), 127.5 (*C*-aromatic), 131.9 (*C*-aromatic), 134.4 (*C*-aromatic), 142.7 (*C*-aromatic), 150.2 (*C*-aromatic) ppm.

ESI-TOF MS (HR MS): calc.: m/z = 676.1600 $[M]^+$; found: m/z = 676.1581 $[M]^+$; error: 2.9 ppm.

Supporting Information

Supporting Information is available from the Wiley Online Library or from the author.

Acknowledgements

The authors thank the Deutsche Forschungsgemeinschaft (DFG, SCHU 1229/30-1; project number: 383067747).

Correction added on October 18, 2021, after initial online publication. A duplicate of this article was published under the DOI 10.1002/macp.202100251. This duplicate has now been withdrawn.

Open access funding enabled and organized by Projekt DEAL.

Conflict of Interest

The authors declare no conflict of interest.

Data Availability Statement

Data are available in article Supporting Information.

Keywords

isothermal titration calorimetry, metallopolymers, selective complexation, supramolecular polymers

Received: August 5, 2021
Revised: August 27, 2021
Published online: September 16, 2021

[1] E. Degtyar, M. J. Harrington, Y. Politi, P. Fratzl, *Angew. Chem., Int. Ed.* **2014**, *53*, 12026.
[2] F. R. Siegel, *Environmental Geochemistry of Potentially Toxic Metals*, Springer, Berlin **2002**.
[3] R. D. M. Hancock, A. E. Martell, *Chem. Rev.* **1989**, *89*, 1875.
[4] R. A. Beauvais, S. D. Alexandratos, *React. Funct. Polym* **1998**, *36*, 113.
[5] S. D. Alexandratos, C. L. Stine, *React. Funct. Polym.* **2004**, *60*, 3.
[6] R. Chakrabarty, P. S. Mukherjee, P. J. Stang, *Chem. Rev.* **2011**, *111*, 6810.
[7] B. H. Northrop, Y.-R. Zheng, K.-W. Chi, P. J. Stang, *Acc. Chem. Res.* **2009**, *42*, 1554.
[8] A. Goswami, M. Schmittel, *Coord. Chem. Rev.* **2018**, *376*, 478.
[9] D. Liu, M. Chen, K. Li, Z. Li, J. Huang, J. Wang, Z. Jiang, Z. Zhang, T. Xie, G. R. Newkome, P. Wang, *J. Am. Chem. Soc.* **2020**, *142*, 7987.
[10] Z. Zhang, Y. Li, B. Song, Y. Zhang, X. Jiang, M. Wang, R. Tumbleson, C. Liu, P. Wang, X.-Q. Hao, T. Rojas, A. T. Ngo, J. L. Sessler, G. R. Newkome, S. W. Hla, X. Li, *Nat. Chem.* **2020**, *12*, 468.
[11] R. Sarkar, T.-Z. Xie, K. J. Endres, Z. Wang, C. N. Moorefield, M. J. Saunders, S. Ghorai, A. K. Patri, C. Wesdemiotis, A. V. Dobrynin, G. R. Newkome, *J. Am. Chem. Soc.* **2020**, *142*, 5526.
[12] S. Chakraborty, G. R. Newkome, *Chem. Soc. Rev.* **2018**, *47*, 3991.
[13] C.-H. Wong, S. C. Zimmerman, *Chem. Commun.* **2013**, *49*, 1679.
[14] L. Shi, X. Wang, C. A. Sandoval, M. Li, Q. Qi, Z. Li, K. Ding, *Angew. Chem., Int. Ed.* **2006**, *45*, 4108.
[15] E. Stulz, Y.-F. Ng, S. M. Scott, J. K. M. Sanders, *Chem. Commun.* **2002**, 524.
[16] M. Schmittel, A. Ganz, *Chem. Commun.* **1997**, 999.
[17] M. Schmittel, V. Kalsani, R. S. K. Kishore, H. Cölfen, J. W. Bats, *J. Am. Chem. Soc.* **2005**, *127*, 11544.
[18] M. Schmittel, B. He, J. Fan, J. W. Bats, M. Engeser, M. Schlosser, H.-J. Deiseroth, *Inorg. Chem.* **2009**, *48*, 8192.
[19] M. L. Saha, S. Neogi, M. Schmittel, *Dalton Trans.* **2014**, *43*, 3815.
[20] M. L. Saha, S. De, S. Pramanik, M. Schmittel, *Chem. Soc. Rev.* **2013**, *42*, 6860.
[21] M. Schmittel, *Isr. J. Chem.* **2019**, *59*, 197.
[22] K. Mahata, M. L. Saha, M. Schmittel, *J. Am. Chem. Soc.* **2010**, *132*, 15933.
[23] J. J. Parlow, *Curr. Opin. Drug Discovery Dev.* **2005**, *8*, 757.
[24] J. Meurer, T. Bätz, J. Hniopek, S. Zechel, M. Schmitt, J. Popp, M. D. Hager, U. S. Schubert, *J. Mater. Chem. A* **2021**, *9*, 15051.
[25] M. S. Özer, A. Rana, P. K. Biswas, M. Schmittel, *Dalton Trans.* **2017**, *46*, 9491.
[26] K. Saalwächter, D. Reichert, in *Encyclopedia of Spectroscopy & Spectrometry*, (Ed: J. Lindon) 2nd ed., Academic Press, London, **2010**, p. 2221.
[27] E. Freire, O. L. Mayorga, M. Straume, *Anal. Chem.* **1990**, *62*, 950.
[28] D. Samanta, I. Paul, M. Schmittel, *Chem. Commun.* **2017**, *53*, 9709.
[29] P. R. Andres, R. Lunkwitz, G. R. Pabst, K. Böhn, D. Wouters, S. Schmatloch, U. S. Schubert, *Eur. J. Org. Chem.* **2003**, *2003*, 3769.
[30] R. S. K. Kishore, V. Kalsani, M. Schmittel, *Chem. Commun.* **2006**, 3690.
[31] L. A. Fulton, W. R. Seitz, R. P. Planalp, *Polyhedron* **2020**, *191*, 114797.
[32] M. Enke, F. Jehle, S. Bode, J. Vitz, M. J. Harrington, M. D. Hager, U. S. Schubert, *Macromol. Chem. Phys.* **2017**, *218*, 1600458.
[33] H. G. Schild, *Prog. Polym. Sci.* **1992**, *17*, 163.
[34] S. Ashraf, H.-K. Park, H. Park, S.-H. Lee, *Macromol. Res.* **2016**, *24*, 297.
[35] Q. Zhang, C. Weber, U. S. Schubert, R. Hoogenboom, *Mater. Horiz.* **2017**, *4*, 109.
[36] T. E. de Oliveira, D. Mukherji, K. Kremer, P. A. Netz, *J. Chem. Phys.* **2017**, *146*, 034904.
[37] S. Furyk, Y. Zhang, D. Ortiz-Acosta, P. S. Cremer, D. E. Bergbreiter, *J. Polym. Sci., Part A: Polym. Chem.* **2006**, *44*, 1492.
[38] J. Meurer, J. Hniopek, T. Bätz, S. Zechel, M. Enke, J. Vitz, M. Schmitt, J. Popp, M. D. Hager, U. S. Schubert, *Adv. Mater.* **2021**, *33*, 2006655.
[39] K. U. Rao, R. M. Appa, J. Lakshmidevi, R. Vijitha, K. S. V. K. Rao, M. Narasimhulu, K. Venkateswarlu, *Asian J. Org. Chem.* **2017**, *6*, 751.
[40] N. S. Lebedeva, Y. A. Gubarev, E. S. Yurina, E. N. Smirnova, S. A. Syrbu, *Colloid Polym. Sci.* **2017**, *295*, 2173.

